

# Positron Lifetime Apparatus and Measurements in Materials

N. J. Elberfeld

May 1, 2006

## Abstract

The theory of positron lifetime spectroscopy is presented. An apparatus is developed to take measurements of positron lifetimes in a variety of materials. Computer programs in Fortran and C are written and edited for analysis of the data. Qualitative observations are made as to the relative purity of materials and the size of the defects within. The system is prepared to take data so that quantitative information can be extracted from the materials. A previously unstudied phenomenon is investigated.

## 1 Introduction

The positron is the anti-particle of the electron, meaning the particles have the same mass and equal but opposite charges. P. A. M. Dirac first postulated the existence of such a particle and C. D. Anderson first observed it in a Wilson cloud-chamber while studying cosmic rays. In theory, a positron could live a very long time in vacuum (average lifetime  $10^{21}$  years), but in material the positron can only live so long as it does not find an electron. One good source,  $Na^{22}$ , emits a positron and then a 1.27 MeV  $\gamma$ -ray 3 picoseconds later. This  $\gamma$ -ray is detectable by scintillators and, because it comes so closely after the positron, is considered to be its “birth” signal [5].

Upon contact with the electron, the pair may bind into a hydrogen-like neutral atom called *positronium*. One state of positronium is the 1S state where  $S=1$ . This is denoted as ortho-positronium (o-Ps). When  $S=0$ , the state is called para-positronium (p-Ps). The two states have approximately the same energy with the latter having slightly less. In vacuum, p-Ps and o-Ps have lifetimes of 125 ps and 142 ns respectively. It is usually the case, however, that because of the low binding energy of the positron, it cannot pick up an extra electron to become positronium. Instead, the positron navigates its way through the material, unable to steal an electron from a “happy” atom. The positron also feels a repulsive force from the positively charged nuclei surrounding it. Thus the positron finds its way to a vacancy where its wave function then overlaps with surrounding electrons’ wave functions and causes it to annihilate. When the positron annihilates, 2 back-to-back 0.511 MeV  $\gamma$ -rays signal the “death” of the positron.

Therefore, the lifetimes of positrons are related to the electron density of the material. By measuring the lifetimes of positrons, information about the electronic structure of a material may be gained: the more electrons, the faster the death of the positron. A lack of electrons (longer lifetimes of positrons) indicates defects such as voids, cracks, holes, or even single atomic vacancies in the substance. The positron lifetime,  $\tau$ , is shown below as a function of the overlap integral of the positron density and the electron density:

$$\frac{1}{\tau} = \pi r_0^2 c \int |\Psi^+(\mathbf{r})|^2 n_-(\mathbf{r}) \gamma d\mathbf{r} \quad (1)$$

where  $\Psi^+(\mathbf{r})$  is the positron wavefunction at  $\mathbf{r}$ ,  $n_-(\mathbf{r})$  is the electron density at  $\mathbf{r}$  before correction for the positronic presence,  $r_0$  is the classical radius of the electron, and  $\gamma$  is a correlation correction to take into account the presence of the positron [2].

$$\gamma = \gamma[n_-(\mathbf{r})] = 1 + \frac{\Delta n_-}{n_-} \quad (2)$$

## 2 Experiment

### 2.1 Apparatus

The overall schematics are given in Figure 1. Positrons from the  $Na^{22}$  source stop in the sample, where the  $\gamma$ -rays then go to the detectors by way of the scintillators. Because the results depend heavily on timing information, plastic scintillators are used to yield the fastest rise time of 0.7 ns. Plastic also has no high  $Z$  material, meaning that the  $\gamma$ -rays are most likely to scatter off of an electron in a process known as the Compton effect. The energies of the scattered photon as determined relativistically are given by the equation:

$$E_\gamma = \frac{1}{\frac{1-\cos(\theta)}{mc^2} + \frac{1}{E_0}} \quad (3)$$

where  $E_0$  is the incident  $\gamma$ -ray energy and  $\theta$  is the scattering angle. The Compton effect is diagrammed in Figure 2.

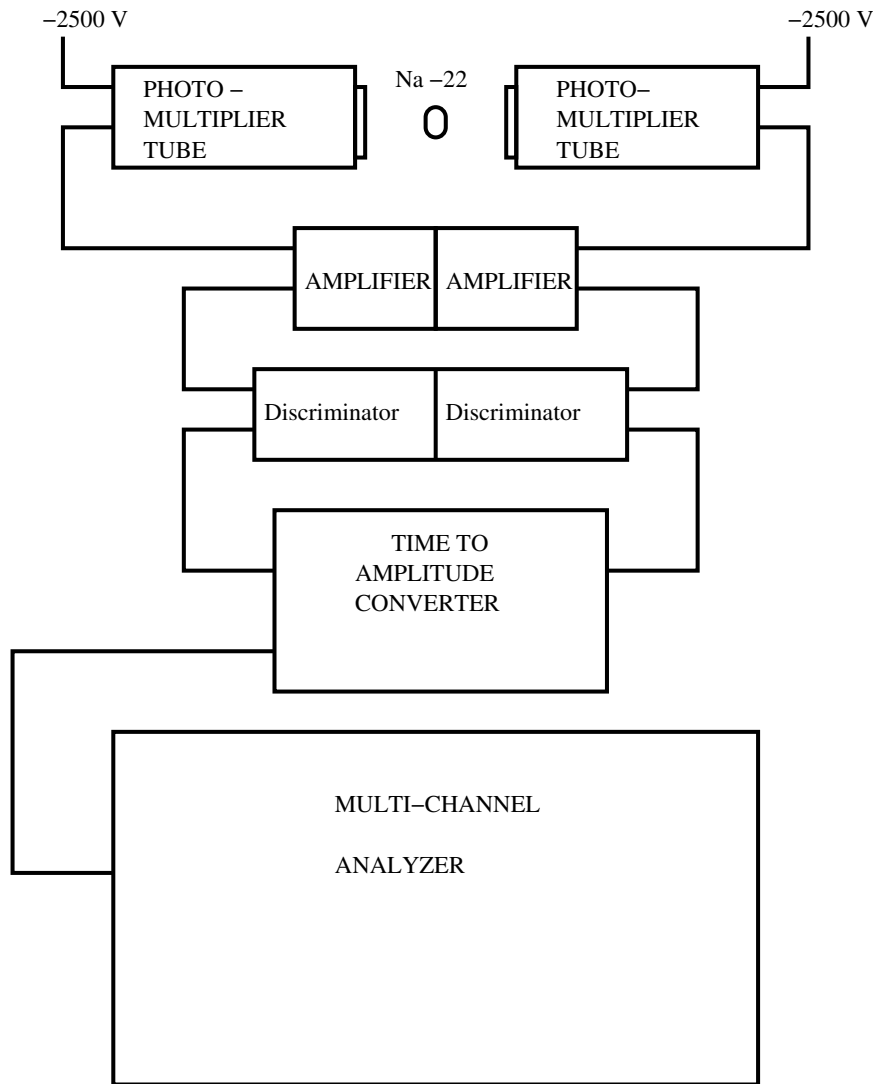


Figure 1: Block Diagram of Experimental Setup.

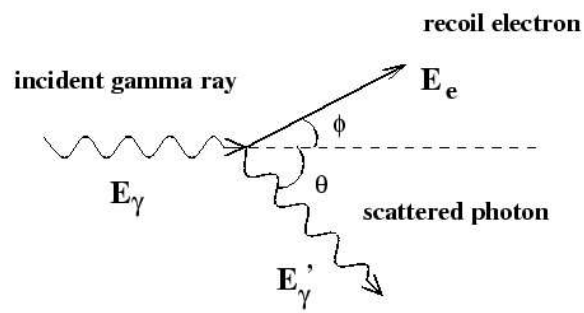


Figure 2: Compton Scattering

Figure 3 shows the energy differential cross sections for 1.27 MeV  $\gamma$ -ray Compton energies convolved with a Gaussian integral to account for statistics. This was determined theoretically by the program “diffxs.f” written in Fortran and attached at the end of the paper.

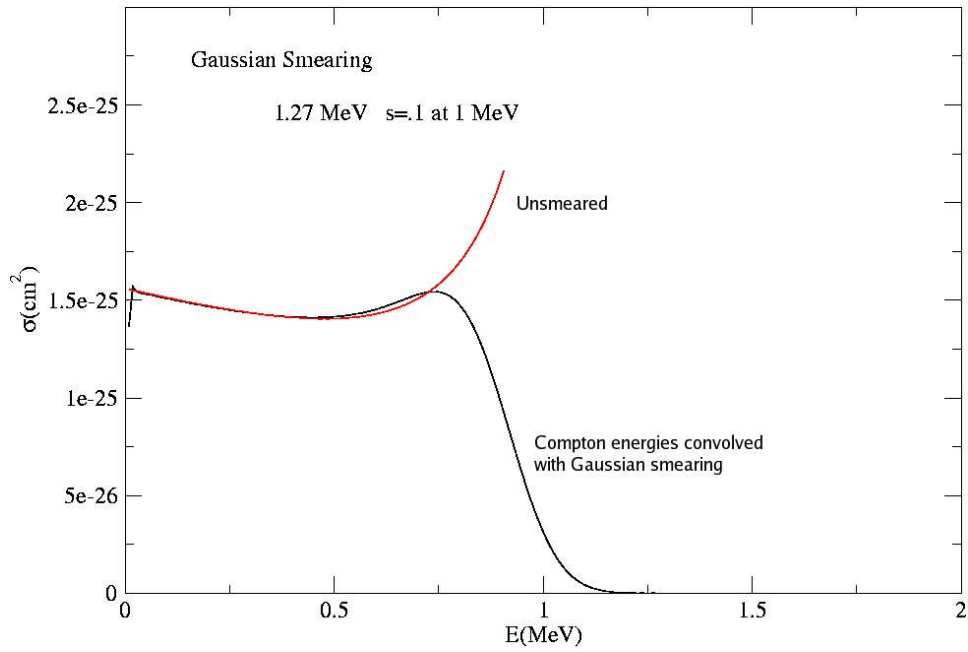


Figure 3: Electron energy distribution for 1.27 MeV photons both with and without convolution with a smearing function.

It is clear from Figure 4 that it is much more efficient to detect the lower, 0.511 MeV  $\gamma$ -rays than the higher 1.27 MeV ones. The relative intensities (roughly 2:1) reflect the fact that there are twice as many 0.511 MeV  $\gamma$ -rays as 1.27 MeV  $\gamma$ -rays. The shape is better fit for the 1.27 MeV  $\gamma$ -ray, indicating perhaps that the smearing is too strong for the 0.511 MeV  $\gamma$ -ray.

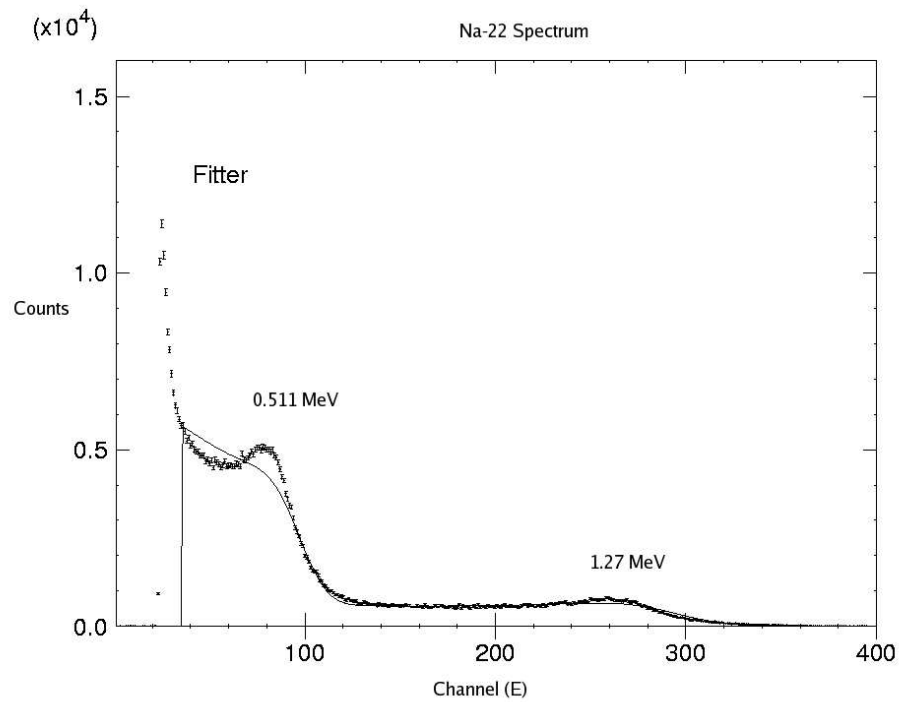


Figure 4: Compton Scattering

The photomultiplier tubes detect these Compton energies and are also very fast. In fact, our Hamamatsu H2431-50 are among the fastest PMTs in the world with rise times of 0.25 ns. These signals are amplified and sent to a constant fraction discriminator which suppresses noise and generates timing pulses. The time to amplitude converter then takes the time difference in pulses (START and STOP) from both sides of the source and converts them into an amplitude which are then stacked into bins in the multichannel analyzer which a computer may use to further analyze.

## 2.2 Computer Analysis

The Spectrum Techniques multi channel analyzer has associated PC software which is used to interface with the hardware apparatus and stores the raw data so that it may be used in fitting programs. The main program to interface with the fitter functions is “fittre.f” (The “English” spelling is used to differentiate it from an older program with a similar name). This latest version incorporates a function that allows parameter data to be written to a file so that it may be recalled by another function. This has greatly improved the gathering and storing of parameter data for a fitted function. The program to take the data and fit it is called “fitf” and has been written in both Fortran and C. The next program of interest is “display.f” also in both languages. This program uses “plplot” to display the data and fitted function. From the Numerical Recipes series, “boiler.f” contains the necessary fitting subroutines. The programs are attached at the end of the paper. The function fits on nine parameters and the fitting parameters are given in channel numbers. By adding an 8 ns delay to the apparatus and observing a 230 channel shift in peak, each channel is observed to be about 35 ps wide.

The function that matches the parameters to the data may be expressed as the following convoluted integral:

$$f(t) = \sum_{i=1}^3 \int_{-\infty}^{\infty} a_i e^{-\frac{(t-t')^2}{2\sigma^2}} e^{-\frac{t'}{\tau_i}} dt' + background \quad (4)$$

The parameters that are fit to this function are  $\sigma$ , the smearing factor,  $a_i$ , the amplitudes of the various convoluted exponentials,  $\tau$ , the lifetimes of the various convoluted exponentials,  $t_0$ , the “zero time” which indicates the channel number corresponding to zero time between the 1.27 MeV  $\gamma$ -ray and the annihilation 0.511 MeV  $\gamma$ -ray, and the background noise (abbreviated “bgnd” in the data tables). The latest version of the fitting program has been adjusted to remove a coupling effect that was taking place between the amplitudes and their respective lifetimes; that is, the amplitude components are now directly related to the number of counts in those bins and thus yield the correct quantitative comparisons needed to analyze the materials effectively.

A typical fitting routine might go as follows:

- 1) Take data into the MCA from the setup diagrammed above.
- 2) Read raw data out into a tab separated variable format (.tsv)
- 3) Remove data heading and list of 0’s read into the low channels

4) Run program "twotothree.f" to take the two columns (channel number, counts) to add a third column of statistical errors (square roots).

5) Run "fittre.f"

The following two letter commands indicate how the fittre program works:

6) rd: read in the data file with 3 columns

7) ra: set range of data

8) ip: input parameter guesses

9) fu: calculate the convolved integral with parameter guesses

10) dl: display log plots of data and fit curve

11) Look at display and re-guess new parameters

12) When the parameter guesses are getting close to the fit, start fitting on a few parameters

13) ft: Fit on specific parameters. Be careful so as not to crash the program with overloading calculations.

14) Once a suitable fit has been obtained (reasonable parameters and lowest  $\chi^2$ ), then save the parameters.

15) wp: write parameters and errors to a file. If the file rd (read in) was called copper.dat, the parameter file will be called parcopper.dat.

16) If old parameters need to be recalled or could be used to help start a new fit, call the old parameters from the parameter file.

17) rp: read the parameters in from, for example, parcopper.dat.

To interpret the results, it is presumed that the longer lifetime components correspond to regions with fewer electrons such as vacancies and voids. Thus a larger amplitude for a longer lifetime component indicates the presence of more defects of that type. In general, the longer the lifetime, the bigger the void type defect.



## 3 Results

### 3.1 $YBa_2Cu_3O_7$ Powder

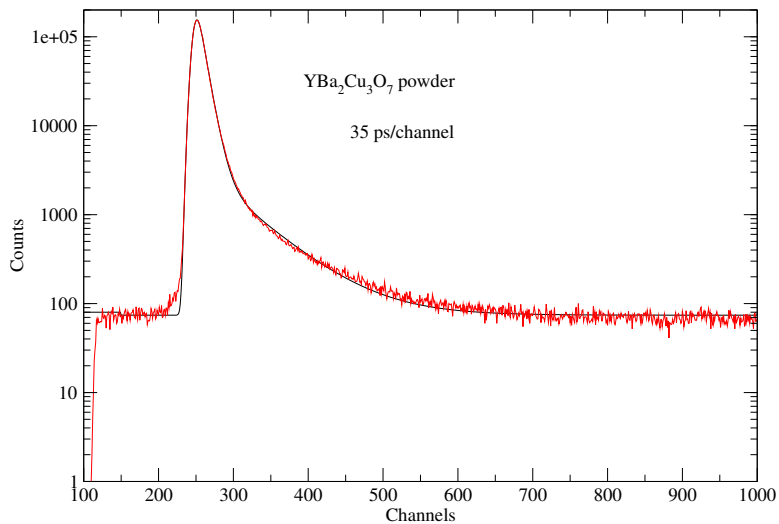


Figure 5: Positron annihilation time spectrum

Table 1: Fitting Data (errors below)

bgnd	$\sigma$	$a_1$	$\tau_1$	$a_2$	$\tau_2$	$t_0$
74.0587	4.69386	234492	8.71543	2566.22	59.6186	246.6
0.3871	5.39E-03	318.11	1.26E-02	26.47	0.3302	7.87E-03

A typical plot of the lifetimes may be seen in Figure 5. The results as determined by the fitting functions attached at the end of the paper are given in Table 6.

This was fit using an earlier program that did not display the third components. A typical fit, the steep right side of the peak represents the shorter  $\tau_1$  component in the absence of defects. This exponential is convolved with the second component which is noticeably longer and corresponds to a longer lifetime while the positron randomly walks in the presence of defects. Where the fit function misses the data to the bottom left of the peak is a curious anomaly. To relate the smearing parameter,  $\sigma$ , to the experimental resolution of the photomultiplier tubes, we use the full width half max (FWHM) equation

$$FWHM = 2\sigma\sqrt{\ln(2)} \quad (5)$$

which yields a value of 274 ps, which is comparable to the best in the literature. When the resolution is very high (meaning the time is very low), then more data can be extracted from under the curve. The lifetimes are easier to see when a large peak is not overlapping with the data.  $\tau_1$  is 270 ps and corresponds to the lifetime of the positron in the electronically stronger material. The  $\tau_2$  value is 2 ns and represents the lifetime in a void. Comparison to other materials brings more insight to these results as it is extremely difficult to calculate what exact sizes and amounts of voids are present given one set of data; that is, the results are meant to be compared to other sets. For example, the ratio of amplitudes does not mean that the sample is 99% pure and 1% defective.

## 3.2 Copper Sample

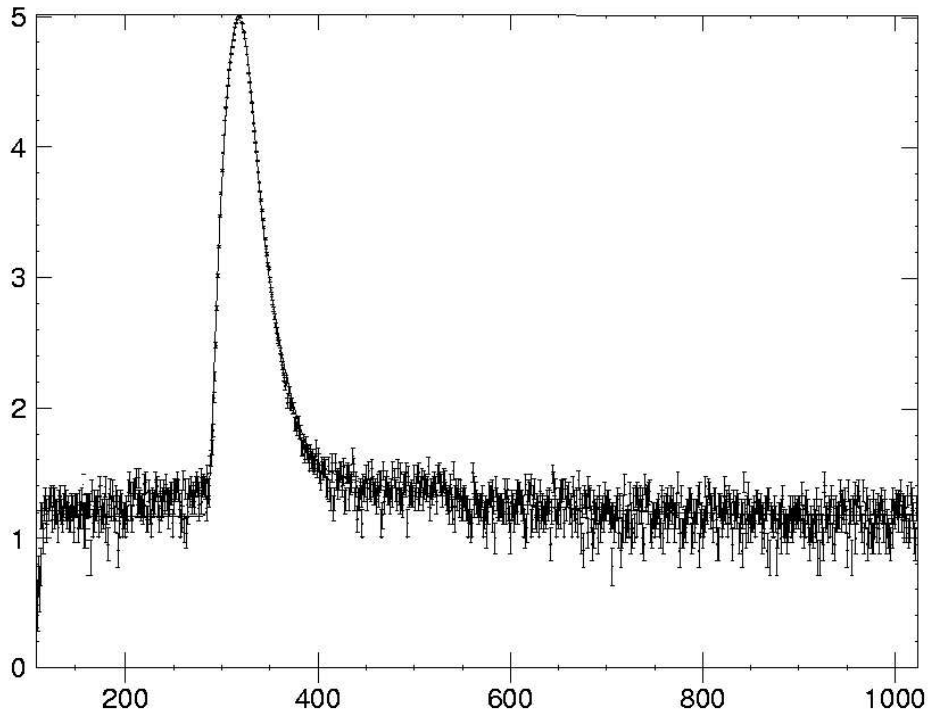


Figure 6: Positron Lifetimes in Copper Sample

Table 2: Copper Fitting Data (errors below)

$\sigma$	$a_1$	$\tau_1$	$a_2$	$\tau_2$	$a_3$	$\tau_3$	bgnd	$t_0$
6.732	1785963.12	4.286	77031.118	14.530	0.	0.	16.3402081	313.925568
0.008	4031.65161	0.030	3824.6792	0.2828	0.	0.	0.15147057	0.02112719

No third component is present in this fit. The shorter lifetime dominates by about a factor of 20. At only .5 ns, the longer lifetime indicates that the rare vacancies are very small.

### 3.3 Iron Sample

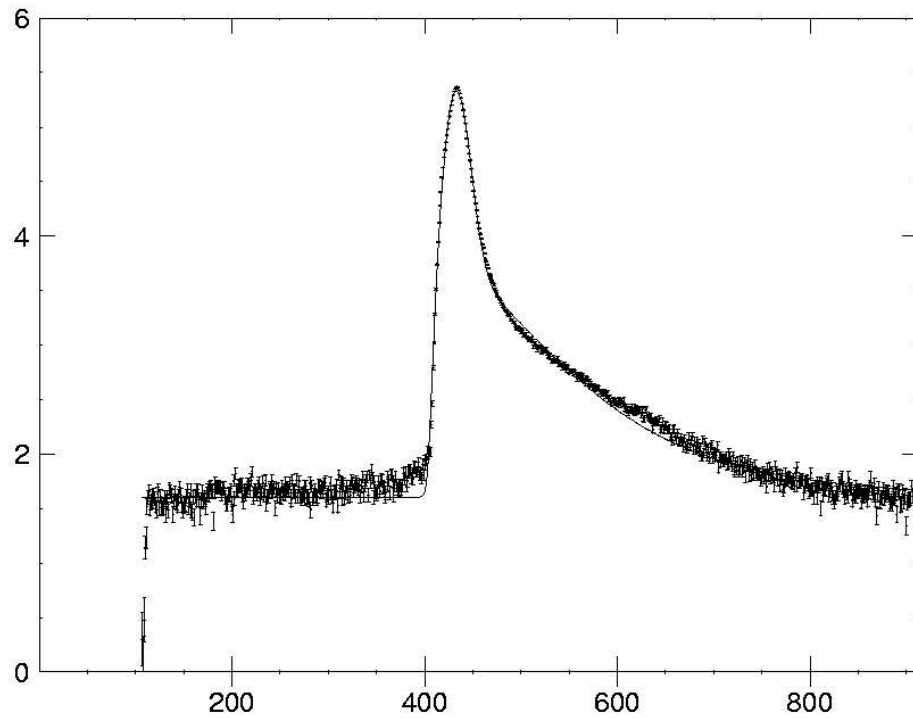


Figure 7: Positron Lifetimes in Iron Sample

Table 3: Iron Fitting Data (errors below)

$\sigma$	$a_1$	$\tau_1$	$a_2$	$\tau_2$	$a_3$	$\tau_3$	bgnd	$t_0$
6.696	4138901.5	4.760	292092.5	41.204792	50631.375	112.805107	40.3479919	429.046051
0.005	2701.6889	0.014	7504.890	0.6107759	8561.9824	5.67820549	0.41499960	0.01178006

As compared to the copper sample, the iron sample has a higher amplitude of the longer second component lifetime which indicates greater amounts of defects. Additionally, the 140 ns lifetime indicates larger defects. At this point, we are unsure as to the physical meaning of the third component amplitude and lifetime.

### 3.4 Magnetic Material Sample

A relatively weak kitchen magnet was used to explore the possibility of an effect on positron lifetimes by the presence of a magnetic field.

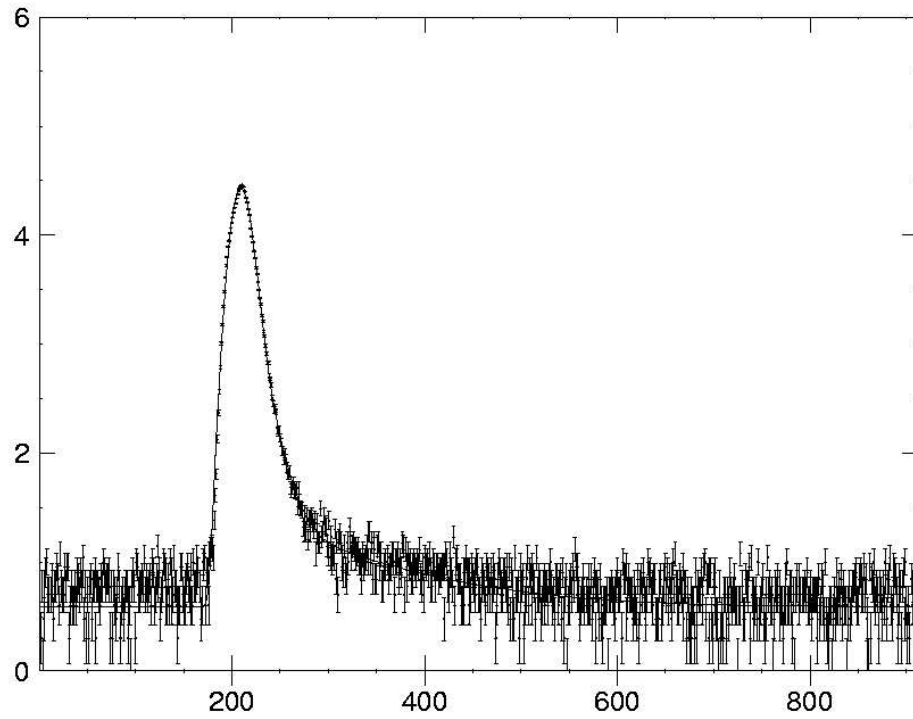


Figure 8: Positron Lifetimes in Magnetic South

Table 4: Magnetic Material South Fitting Data (errors below)

$\sigma$	$a_1$	$\tau_1$	$a_2$	$\tau_2$	$a_3$	$\tau_3$	bgnd	$t_0$
7.355	524103.562	4.102	43186.14	12.066	2366.954	110.668	3.836	205.677
0.019	5555.690	0.097	4540.915	0.5975	1417.522	10.433	0.109	0.05793

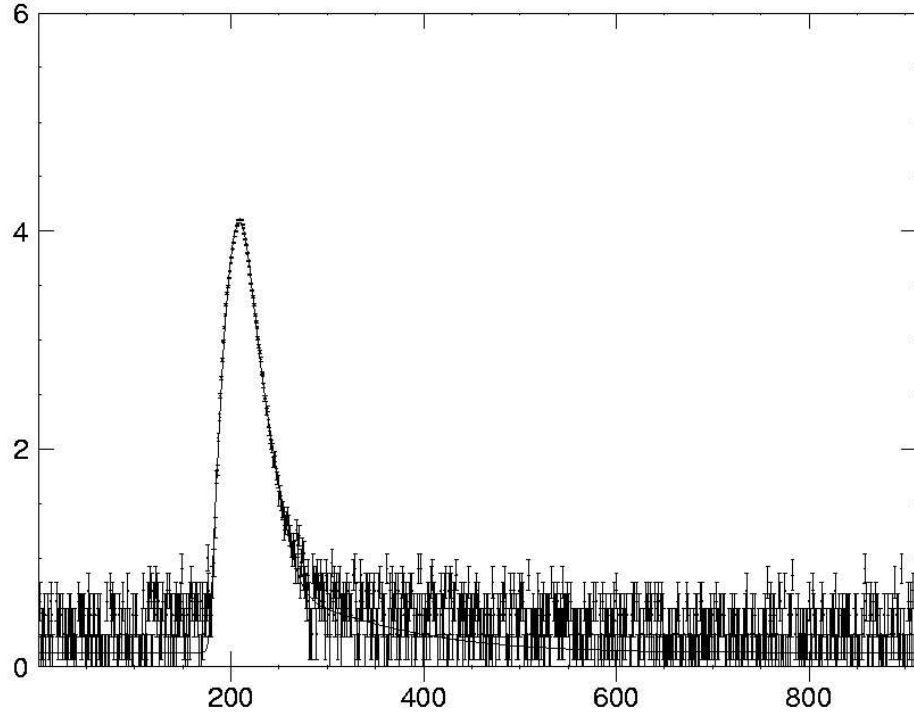


Figure 9: Positron Lifetimes in Magnetic North

Table 5: Magnetic Material North Fitting Data (errors below)

$\sigma$	$a_1$	$\tau_1$	$a_2$	$\tau_2$	$a_3$	$\tau_3$	bgnd	$t_0$
7.006	169894.29	0.972	58693.48	7.513	507.593	88.907	1.349	207.340
0.089	5646.6870	0.937	9799.427	0.174	4405.75	17.921	0.059	0.86578

The discrepancies between data from the north and south orientation of the same magnets is potentially very interesting. Notice that the lifetimes in the north set are significantly shorter than in the south set. This phenomenon will be explained in greater detail in the next section.

## 4 Developing Studies and Conclusions

### 4.1 Quantitative Analysis

So far, we have successfully implemented fitting functions to interpret data from several runs. We hope to run far more experiments and do comparative analysis on radiation damaged samples (probably from the beam dump at JLAB). Ideally, the setup can become a commissioning study so that one could do work for NASA. While some analysis has yielded interesting qualitative insight, many more systematic comparisons must be made to extract meaningful quantitative information from the system. With so much work this year going into tweaking the apparatus and writing and editing the various computer programs that must accompany the hardware, the setup is nearly ready for such rigorous studies.

### 4.2 Positron Lifetime in a Strong Magnet

As described in the introduction, positrons may form *positronium* when their wave functions overlap with that of the electrons. Depending on the orientation of the spins, this will either be ortho- or para-positronium (o-Ps, p-Ps respectively). In a permanent magnet, most of the strength in its magnetic field is due to unmatched (un-canceled) spins of electrons. One such magnet, neodymium iron boron, or *NdFeB* has a partially occupied *f* electron shell and as such may have up to 14 aligned spins. If larger than a penny, some of these magnets can lift over 10 kilograms. The spins from the aligned electrons in this shell would then interact with the conduction electrons in a quantum-mechanical phenomenon known as “exchange coupling.” This would allow the conduction electrons that the positron sees to become polarized and thus effect the lifetime results. We have not been able to find any previous positron lifetime studies on the dependence on magnetization direction with respect to the positronic polarization and thus further pursuit of this topic may be worthy of publishing.

## 5 Acknowledgments

From particle physics to “LaTeXing”, undertaking this thesis has improved my understanding of both science and the scientific process. There exists a large gap (infinite square well, perhaps?) between fulfilling an experiment in one class period and working from scratch for a year or more. Whether checking thresholds, adjusting amplification, forgetting that the voltage is turned off and wondering what could possibly be wrong, or trying to learn computer languages and operating systems, every component of a unified system becomes an individual experiment. Unfortunately, such frustrations may be to the exclusion of copious amounts of data and results; I was hoping to take several more runs to extract more quantitative information. Simultaneously, such is the reality of real science and thus the experience is as invaluable to the young scientist as are the results. Finally, I want to thank Dr. William J. Kossler for his time and patience in helping me. Professor, mentor, good conversationalist, and avid tennis-player, this work would not have been possible for me to

explore without his guidance. I would like to see this study continued, if not by me this summer, then by future seniors eager to understand the process of science.



## References

- [1] P. A. M. Dirac. The Quantum Theory of the Electron. *Proceedings of the Royal Society A*, 117:610, 1928.
- [2] <http://positrons.physics.lsa.umich.edu/home.html>
- [3] April H. Baugher. *Microstructural Characterization of an Ultra-High Performance Polyimide..* PhD thesis, College of William and Mary, 1997.
- [4] C. D. Anderson. The Positive Electron. *Physical Review*, 43:491, 1933.
- [5] Lederer, Hollander, and Perlman. *Table of Isotopes*. John Wiley & Sons, New York, sixth edition, 1967.